Available online at www.sciencedirect.com
ScienceDirect
Journal of Sound and Vibration 305 (2007) 116–133
JOURNAL OF SOUND AND VIBRATION
www.elsevier.com/locate/jsvi

Application of multivariate uncertainty analysis to frequency response function estimates

Todd Schultz, Mark Sheplak, Louis N. Cattafesta III*

Interdisciplinary Microsystems Group, Department of Mechanical and Aerospace Engineering, University of Florida, Gainesville, FL 32611-6250, USA

Received 10 August 2005; received in revised form 16 March 2007; accepted 21 March 2007

Abstract

Uncertainty estimation is an important part of any measurement but is often neglected for complex valued or multivariate data (e.g., vectors). This paper presents a methodology for estimating the uncertainty in multivariate experimental data and applies it to the measurement of the frequency response function obtained when using a periodic random input signal. This multivariate uncertainty method is an extension of classical uncertainty methods used for scalar variables and tracks the correlation between all variates along with the sample variance instead of just tracking the standard uncertainty. The method is used in this paper to propagate the sample covariance matrix from spectral density estimates to the uncertainty in the frequency response function estimate for two different system models. In the first model the case when only the output signal is corrupted by noise is considered, while in the second model both the input and output signals are corrupted by uncorrelated noise sources. The results for the single-noise model are verified by comparing them to published expressions in the literature, while the results for the two-noise model are verified by using a direct computation of the statistics. Finally, the method is applied to experimental data from two microphone measurements within an acoustic waveguide. The random uncertainty estimates in the frequency response function from the multivariate method agree well with the results from a direct computation of the statistics.

1. Introduction

Linear, time-invariant systems occur in many engineering applications and are completely characterized by a frequency response function. Examples applications include digital and analog filters, and acoustic impedance measurements. Measurements of the frequency response function are commonly performed to test unknown systems and verify analytical models, but knowledge of the uncertainty in the estimated frequency response function is also desirable, if not essential. The advent of inexpensive and powerful microprocessors has made estimation of frequency response functions utilizing the fast Fourier transform algorithm routine. Use of Gaussian random noise as input prompted research on the associated measurement uncertainty in the frequency response function [1], spectral leakage [1,2], the development of specialized window functions [3],

*Corresponding author. Tel.: +1 353 846 3017; fax: +1 352 392 7303.
E-mail address: cattafes@ufl.edu (L.N. Cattafesta III).

0022-460X/$ - see front matter © 2007 Elsevier Ltd. All rights reserved.
doi:10.1016/j.jsv.2007.03.084

and the use of periodic input signals to eliminate leakage [4–7]. Where possible, the use of a periodic random (or pseudo-random) noise input is acknowledged as the preferred approach to eliminate bias errors in the frequency response function associated with spectral leakage, but the random errors associated with such an input differ from those in the corresponding white noise input case. Indeed, modern spectrum analyzers now incorporate these features but do not provide an estimate of the measurement uncertainty. The contribution of this paper is to demonstrate a multivariate statistical methodology for estimating the random uncertainty in the frequency response function estimate when using a periodic random noise input. Two different system models are considered, one with noise only on the output signal and the other with uncorrelated noise on both the input and output signals.

The multivariate uncertainty method is by no means the only method to estimate uncertainty in a complex quantity. An alternative method is the complex statistics approach outlined in Refs. [4,5,8], which represents the sample standard deviation of a complex number with a single real-valued number via the circular complex random variable assumption. A circular complex random variable is a random variable of a complex quantity with symmetrical normal distributions for the real and imaginary parts with the same variance [8]. Thus, the confidence region is a circle in the complex plane [5]. The basis for this approach is that when the discrete Fourier transform is used to transform data from the time to the frequency domain, the spectral lines have asymptotic circular normal distributions. Hence, the single variance may be used because the correlation between the real and imaginary part is zero.

In contrast, a multivariate uncertainty analysis treats the complex random variable as a bivariate normal random variable that allows different values of variance for each variate and a covariance. The elimination of the complex random variable assumption can result in an elliptical confidence region, but this flexibility comes at the cost of increased mathematical complexity. The main advantages of the multivariate uncertainty analysis are as follows. First, it is applicable to other higher-dimensional data, such as velocity vectors and multiple-input, multiple-output systems. Second, it estimates the frequency response function uncertainty within a framework based on linear perturbations similar to that given in the Guide to the Expression of Uncertainty in Measurements published by the International Organization for Standardization [9]. Third, the method is easily adapted to different frequency response function estimators and can be used to propagate the frequency response function uncertainty through a subsequent data reduction equation without the circular complex random variable assumption [8].

The outline of the paper is as follows. Section 2 contains a brief review of classical uncertainty analysis, which sets the stage for a discussion of multivariate methods. The section also includes a simple demonstration of the multivariate method by converting the uncertainty in real and imaginary parts of a complex variable to magnitude and phase. In Section 3, expressions for the random uncertainty in the frequency response function estimate when using a periodic random input for the two system models mentioned above are given to differentiate between the effects of input and output noise on the uncertainty. The results for the single-noise model are verified by comparing them to published expressions in the literature [1], while the results for the two-noise model are verified by using a direct computation of the statistics. The multivariate uncertainty method is then applied to data from an acoustic application that requires the measurement of the frequency response function between two microphones.

2. Uncertainty analysis

Experimental data analysis consists of two parts: estimating the measured quantity and the corresponding uncertainty. The estimate of the measured quantity, called the *measurand*, is an estimate of the true value of the quantity. The uncertainty quantifies the estimated accuracy in terms of a confidence interval [10].

Many articles and books have been published outlining methods to estimate uncertainty in experimental data. One of the first publications, by Kline and McClintock in 1953 [10], was revisited in 1983 by the ASME Symposium on Uncertainty Analysis and published in the Transactions of the ASME in 1985 [11]. Currently, the many texts available on the subject include the ISO Guide [8], the *NIST Technical Note* 1297 by Taylor and Kuyatt [12], and *Experimentation and Uncertainty Analysis for Engineers* by Coleman and Steele [13]. All these publications prescribe essentially the same procedure, which is summarized in the next section, but they vary

slightly in the philosophy of the uncertainty source classification. In this paper, uncertainty sources are classified as random and bias [10,11,13] as opposed to Type A and Type B [8,12].

The approaches to uncertainty analysis described in Refs. [8,10–13] are limited to scalar or real-valued data. These methods do not apply to data that are multidimensional or *multivariate*. Multivariate data have multiple, possibly correlated, components. Examples of multivariate data include measurements of vector quantities and complex-valued data such as frequency response functions. Relevant examples using multivariate uncertainty analysis that parallels classical work are presented in Refs. [14–17].

2.1. Classical uncertainty analysis

The classical uncertainty method described in Refs. [8,10–13] estimates the uncertainty associated with a data reduction equation by using a first-order Taylor-series expansion. Thus, the uncertainties of the input variables must be small enough such that they do not violate the local linear approximation. The uncertainty propagation equation for the standard uncertainty or sample standard deviation, u_r, is

$$u_r = \sqrt{\sum_{i=1}^{n} \left(\theta_i u_{x_i}\right)^2 + 2\sum_{i=1}^{n-1}\sum_{j=i+1}^{n} \theta_i \theta_j u_{x_i x_j}}, \tag{1}$$

where u_{x_i} is the standard uncertainty or sample standard deviation of the ith input variable, $u_{x_i x_j}$ is the sample covariance between the ith and jth input variables, and $\theta_i = \partial r/\partial x_i$ is the sensitivity coefficient. The confidence interval is estimated by multiplying u_r by a coverage factor, k, that is a function of the distribution of the variable and the confidence level desired. Methods for computing the coverage factor based on the t-distribution are given in Refs. [8,12,13]. Moffat provides an extension to the above classical method by eliminating the requirement of computing the derivatives analytically via numerical approximations [18]. Another subtlety in the classical method is that the underlying statistical distributions of the input variables are not propagated in the analysis. Therefore, one must assume a form of the distribution in order to complete the uncertainty analysis and estimate the confidence interval. Monte Carlo methods offer an alternative to assuming a distribution but are computationally expensive [13]. In spite of these issues, classical uncertainty analysis provides a way to estimate a confidence interval for experimental data and can be used before any measurements are taken for experimental design purposes.

2.2. Multivariate uncertainty analysis

Multivariate uncertainty analysis extends classical methods to multivariate problems via systematic use of the correlation between variates both in the input and output variables.

2.2.1. Fundamentals

Before outlining the procedure for multivariate uncertainty analysis, some general information is needed. First, a multivariate problem with p variates will have p^2 uncertainty components, but not all the components are independent due to the symmetry of the covariance matrix [19]. Thus, the covariance matrix will have only $p(p+1)/2$ independent elements. The task of the multivariate uncertainty analysis is to propagate the covariance matrix through the data reduction equation. The result is another covariance matrix that represents the variation in the calculated output variables.

Complex-valued data can be thought of as *bivariate* because each variable has *two* parts. The two parts of any complex variable can be represented in either real and imaginary or magnitude and phase forms. All complex computations of the quantity in question and its uncertainty are performed with the real and imaginary parts. The advantage is that the real and imaginary axes extend to infinity in both directions as compared to the magnitude and phase axes, in which the magnitude is constrained to be a positive real number, and the phase lies between -180° and $+180^\circ$. This forces the use of modular arithmetic for the polar form that can influence the prediction of the uncertainty [16]. The rectangular form for the complex estimate and uncertainty can be converted to polar form for final display as is customary for frequency response function, but only the rectangular form of the estimate and uncertainty should be propagated.

In addition to complex-valued variables, another difference compared to the classical method is that a confidence interval is now extended to multidimensional space. For bivariate data, the confidence interval is extended to a confidence area. The shape of the confidence area is a function of the uncertainty in each of the variates and the correlation between them. For a multivariate normally distributed variable, the confidence region is defined by first considering the probability statement [19]:

$$\mathrm{Prob}\left((\mathbf{x}-\bar{\mathbf{x}})^T\mathbf{s}^{-1}(\mathbf{x}-\bar{\mathbf{x}})\leqslant\frac{v_{\mathrm{eff}}p}{v_{\mathrm{eff}}+1-p}F_{p,v_{\mathrm{eff}}+1-p,\alpha}\right)=1-\alpha, \tag{2}$$

where $\mathbf{x}$ is a vector representing the multivariate variable, $\bar{\mathbf{x}}$ is the sample mean vector, $\mathbf{s}$ is the sample covariance matrix, $F_{p,v_{\mathrm{eff}}+1-p,\alpha}$ is the statistic of the F distribution with p, $v_{\mathrm{eff}}+1-p$ degrees of freedom and a probability $1-\alpha$, $\alpha\leqslant 1$ is the level of significance, p is the number of variates, and v_{eff} is the effective number of degrees of freedom in the measurements. For a single random variable, the effective number of degrees of freedom is the number of measurements less one. Otherwise, Willink and Hall discuss in detail how to estimate the effective number of degrees of freedom [17]. The method estimates the effective degrees of freedom by matching the generalized variances for all the input variates and reduces to the Welch–Satterhwaite method for a univariate problem. The Welch–Satterhwaite is the method recommended to estimate the effective number of degrees of freedom in Refs. [8,12].

Application of Eq. (2) for a complex variable results in a confidence region that is an ellipse. If x_R and x_I are the real and imaginary parts of a complex variable, respectively, then the confidence region is given by

$$\left(\frac{x_R-\bar{x}_R}{u_{x_R}}\right)^2-2\rho\frac{x_R-\bar{x}_R}{u_{x_R}}\frac{x_I-\bar{x}_I}{u_{x_I}}+\left(\frac{x_I-\bar{x}_I}{u_{x_I}}\right)^2\leqslant(1-\rho^2)\frac{v_{\mathrm{eff}}p}{v_{\mathrm{eff}}+1-p}F_{p,v_{\mathrm{eff}}+1-p,\alpha}, \tag{3}$$

where u_{x_R} and u_{x_I} are the sample standard deviations of x_R and x_I, respectively, and ρ is the correlation coefficient, defined as

$$\rho=\frac{E[(x_R-\bar{x}_R)(x_I-\bar{x}_I)]}{u_{x_R}u_{x_I}}, \tag{4}$$

where $E[\,]$ is the expectation operator. From Eq. (3), the simultaneous uncertainty bounds on the real and imaginary parts are given by the projections of the ellipse onto the respective axis and the correlation determines the orientation of the ellipse. For the case of no correlation, $\rho=0$, the axes of the ellipse are aligned with the real and imaginary axes. For the case of perfect correlation, $\rho\to\pm 1$, the ellipse collapses to a line. This is intuitive because, if the two variates are perfectly correlated, then only knowledge of one of them is required to determine the other variable.

If the entire confidence region is not desired, the simultaneous confidence interval estimates of the uncertainty for each variate can be computed from

$$U_n=ku_n, \tag{5}$$

where u_n is the estimate of the sample standard deviation for the nth variate, and k is the coverage factor given by

$$k=\sqrt{\frac{v_{\mathrm{eff}}p}{v_{\mathrm{eff}}+1-p}F_{p,v_{\mathrm{eff}}+1-p,\alpha}}. \tag{6}$$

The F-distribution is necessary to accommodate the correlated multiple dimensions since the population distribution is assumed to be a multivariate normal distribution [16,19]. For the remainder of this paper, the coverage factor will be computed using two variates for complex data and the number of spectral records minus one. Thus, the uncertainty reported for one of the variates would be $x_n\pm U_n$, and a corresponding expression can be written for each variate.

2.2.2. Multivariate uncertainty propagation

The task of the multivariate method for uncertainty analysis is to propagate the uncertainty estimates through a data reduction equation. The difference between this and the classical method is that the

multivariate method simultaneously computes the uncertainty estimates for each variate along with the correlation between them, while the univariate approach only estimates the uncertainty for a single variable. Consider a generalized data reduction equation of the form

$$\vec{r} = r\left(\vec{x}\right), \tag{7}$$

where $\vec{r}$ is the real-valued vector of output variates, and $\vec{x}$ is the real-valued vector containing all input variates. Note that any data reduction equation that has multiple input variables can be recast in the form of a single input variable with multiple variates. The first step is to create a separate expression for each output variate $r_1, ..., r_p$ and then form the Jacobian matrix

$$\mathbf{J} = \begin{bmatrix} \frac{\partial r_1}{\partial x_1} & \frac{\partial r_1}{\partial x_2} & \cdots & \frac{\partial r_1}{\partial x_p} \\ \frac{\partial r_2}{\partial x_1} & \frac{\partial r_2}{\partial x_2} & \cdots & \frac{\partial r_2}{\partial x_p} \\ \vdots & \vdots & \ddots & \vdots \\ \frac{\partial r_p}{\partial x_1} & \frac{\partial r_p}{\partial x_2} & \cdots & \frac{\partial r_p}{\partial x_p} \end{bmatrix}, \tag{8}$$

where the subscript denotes the variate. The uncertainty propagation equation now takes the form [14–17]

$$\mathbf{s}_r = \mathbf{J}\mathbf{s}_x\mathbf{J}^{\mathrm{T}}, \tag{9}$$

where $\mathbf{s}_r$ is the sample covariance matrix for the output variable, and $\mathbf{s}_x$ the sample covariance matrix for the input variable. If Eq. (9) is used for a univariate output, the result identically matches the expression given in Eq. (1) for the classical uncertainty analysis method. The limitations and remedies of the multivariate uncertainty analysis are the same as those for the classical uncertainty analysis discussed above and include linearization and numerical approximations.

2.3. Application: converting uncertainty from real and imaginary parts to magnitude and phase

The multivariate uncertainty method is now demonstrated for converting complex-valued data from real and imaginary parts to magnitude and phase. For this example, the true mean value is $x_{\mathrm{true}} = 4 + \mathrm{j}3 = 5\mathrm{e}^{\mathrm{j}0.644}$, and the population covariance matrix is

$$\mathrm{cov}\left(x_{\mathrm{true},R}, x_{\mathrm{true},I}\right) = \begin{bmatrix} 0.01 & 0.0021 \\ 0.0021 & 0.0049 \end{bmatrix}. \tag{10}$$

The population distribution is a bivariate normal distribution. The sample covariance matrix is estimated from ten random data samples, and the uncertainty is propagated to the magnitude and phase by using Eq. (9). Also, each of the ten data points are converted to a polar representation, and the output sample covariance matrix of the magnitude and phase are calculated directly. The estimates of the output sample covariance matrix are then compared to illustrate the effectiveness of both methods. To conclude the example, the coverage factor is computed and the confidence region is plotted by using Eq. (3), along with a scatter plot of the data.

The sample mean of the real and imaginary parts of the data are 4.01 and 3.04, respectively. The raw data are plotted in Fig. 1 along with the sample mean value, the population mean value and the estimate of the 95% confidence region around the sample mean value. The computed coverage factor from Eq. (6) is 3.08. Note that the major and minor ellipse axes are not parallel to the respective coordinate axes due to the correlation between the two variates. The figure shows that the estimated confidence region contains the true value of the population mean.

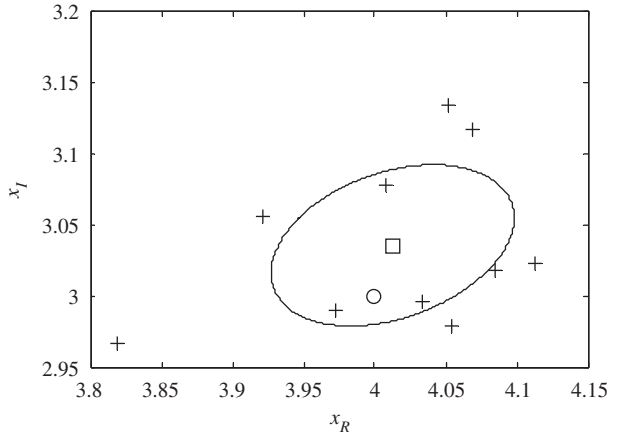

Fig. 1. A plot of the raw data and estimates for a randomly generated complex variable. +, Data points, □, estimated mean value, ○, true value, ——, 95% confidence region.

Now that the sample covariance matrix and the uncertainty region are computed and verified for the real and imaginary parts, the uncertainty can also be propagated to the magnitude and phase. The Jacobian matrix becomes

$$\mathbf{J} = \begin{bmatrix} \dfrac{\partial|x|}{\partial x_R} & \dfrac{\partial|x|}{\partial x_I} \\ \dfrac{\partial(\angle x)}{\partial x_R} & \dfrac{\partial(\angle x)}{\partial x_I} \end{bmatrix} = \begin{bmatrix} \dfrac{x_R}{\sqrt{x_R^2+x_I^2}} & \dfrac{x_I}{\sqrt{x_R^2+x_I^2}} \\ -\dfrac{x_I}{x_R^2+x_I^2} & \dfrac{x_R}{x_R^2+x_I^2} \end{bmatrix}. \tag{11}$$

The Jacobian matrix, evaluated at the sample mean values, and Eq. (9) is used to propagate the standard uncertainty. The sample covariance matrix computed from Eq. (9) is

$$\mathbf{s}_{\text{polar,propagated}} = \begin{bmatrix} 0.783 & -0.0322 \\ -0.0322 & 0.0130 \end{bmatrix} \times 10^{-3} \tag{12}$$

and the sample covariance matrix computed directly from the 10 sample data points in polar form is

$$\mathbf{s}_{\text{polar,direct}} = \begin{bmatrix} 0.782 & -0.0335 \\ -0.0335 & 0.0130 \end{bmatrix} \times 10^{-3}. \tag{13}$$

The element (1,1) in Eqs. (12) and (13) represents the variance in the magnitude, and element (2,2) represents the variance in the phase. The off-diagonal element gives the covariance between the magnitude and phase. The difference between any two corresponding elements in the two estimates for the sample covariance matrix is less than 5%. The data, the mean values, and the uncertainty estimates are shown in Fig. 2, where again the true value is contained within the confidence region. The computed coverage factor from Eq. (6) that was applied to the estimates of the standard uncertainty to compute the 95% confidence estimates is 3.08. The estimated values for the magnitude and phase with uncertainties are $|\overline{x}| = 5.03 \pm 0.09$ and $\angle\overline{x} = 0.648 \pm 0.011$ [rad]. This simple example demonstrates the usefulness of the multivariate uncertainty analysis and provides some insight concerning the terms and concepts described above.

This example demonstrated how the correlation between the uncertainty in the real and imaginary components propagated to yield correlated uncertainties in the magnitude and phase. In many applications, including the estimation of spectral density functions, the uncertainty in the magnitude and phase are assumed to be uncorrelated. However, this is not always the case, particularly at low signal-to-noise ratios. In any case, care should be taken when propagating the uncertainty. The uncertainty should only be propagated in rectangular form, and the uncertainties in the magnitude and phase should only be used for final display purposes.

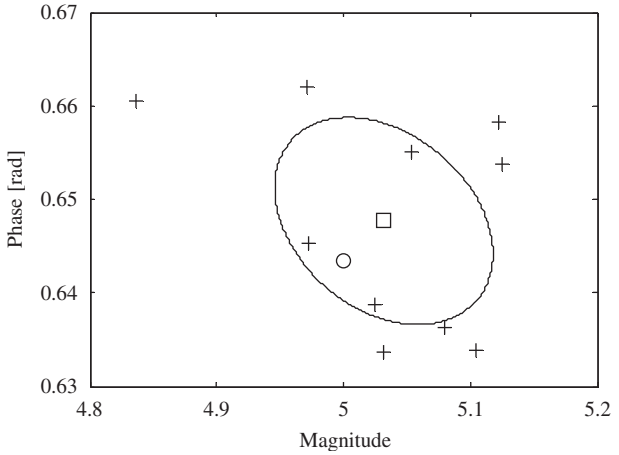

Fig. 2. A plot of the raw data and estimates in polar form for a randomly generated complex variable. +, Data points, □, estimated mean value, ○, true value, ——, 95% confidence region.

3. Frequency response function estimates

The frequency response function is ubiquitous in engineering systems, yet the measurement and estimation of its uncertainty is nontrivial. There are many factors to consider when measuring and estimating a nonparametric frequency response function, such as the analog-to-digital sampling settings, the fast Fourier transform settings, the assumption of a system model describing the way noise enters the signals, etc. Previous researchers have studied techniques for reducing the error in the frequency response function but few have studied the uncertainty in the final estimate. Bendat and Piersol [1], Schmidt [2] and Pintelon et al. [6] have derived expressions for the uncertainty in the frequency response function for some cases. This paper, however, provides a systematic framework involving periodic deterministic inputs and propagation of the resulting uncertainty to derived quantities. The random uncertainty for two system models and the data reduction equations for estimating the frequency response function are analyzed by using a multivariate uncertainty analysis framework. The first model is a single-input/single-output system with Gaussian noise added only to the output signal, which is relevant for system identification applications involving a noise-free input signal and a (perhaps) noisy output sensor signal. The expressions derived by the multivariate method are compared to the results given in Bendat and Piersol [1]. The second model is another single-input/single-output system, but uncorrelated Gaussian noise signals are added to both the input and output signals. This system model is representative of the case in which the frequency response function is estimated between two microphones such as in the two microphone method used to measure acoustic impedance in an acoustic plane wave tube. The measured "noise" signals without any excitation are typically uncorrelated in this scenario. The results of this case are compared to numerical simulations designed to verify the derived uncertainty expressions.

The systems studied in this paper are assumed to be excited by a periodic random input signal. This type of signal, which is standard in most modern spectrum analyzers, is tailored to the parameters chosen for the spectral analysis and designed to prevent spectral leakage. An example of this type is called pseudo-random noise [20]. This signal is actually deterministic and consists of a finite summation of discrete sine waves at the frequencies in the spectral analysis, but each component has a random, uniformly distributed phase angle. The probability density function for the pseudo-random signal approaches a Gaussian distribution as the number of components is increased. In practice, the distribution can be approximated as Gaussian if 400 or more discrete sine waves are used. The periodicity of the input signal prevents any bias error in the estimated spectrum due to spectral leakage when a uniform or boxcar window is used of duration equal to one period of the excitation signal; thus the remainder of this paper assumes that there is no bias uncertainty due to leakage in the spectral estimates.

3.1. Output noise only system model

The first system model is illustrated in Fig. 3, where x is the pseudo-random input signal, v is the noise-free output of the system, n is a zero-mean, Gaussian noise signal, y is the measured output, $H(f)$ is the frequency response function of the linear system, and f is the frequency. For this case, the noise signal models all measurement noise and also includes the response to unmodeled system inputs. This model is appropriate for linear systems where noise in the input signal is negligible, such as when an input signal is from a function generator in, for example, system identification and open-loop control system applications. This is because many function generators have a dynamic range approximately 40 dB higher than a typical signal analyzer.

The time-domain output signal is the sum of the noise-free output signal, $v(t)$, which is periodic because the system is at steady state, and a stationary noise signal, $n(t)$,

$$y(t) = v(t) + n(t) = h(t)^* x(t) + n(t), \tag{14}$$

where t is time, $h(t)$ is the impulse response function, and "*" denotes the convolution. Let $N(f_k, T)$ denote the discrete Fourier transform of T seconds of the noise signal sampled at f_s samples per second, where $f_k = k/T$ denotes the discrete frequencies. Also, note that $X(f_k, T)$, $V(f_k, T)$, and $Y(f_k, T)$ are defined similarly, although $V(f_k, T)$ cannot be computed since $v(t)$ is not available. Because of the periodic nature of the noise-free output at steady state, the discrete Fourier transform of exactly one period (T seconds) gives

$$Y(f_k, T) = V(f_k, T) + N(f_k, T) = H(f_k)X(f_k, T) + N(f_k, T) \tag{15}$$

if there was no aliasing in the sampling process. Here, $H(f_k)$ is the system frequency response function, i.e. the Fourier transform of the system impulse response, $h(t)$, evaluated at f_k. Each period in the response time history yields a sample record of the ensemble used to estimate the auto- and cross-spectral density functions [1]. Note that Bendat and Piersol in Ref. [1] use $N(f)$ to denote the Fourier transform of T seconds of $n(t)$.

Eq. (15) and the Fourier transform of the input signal, $X(f_k, T)$, are substituted into the definitions of the auto- and cross-spectrum density functions [1]. In the analysis, the following well known statistical results are used. Consider two random variables $\tilde{A}$ and $\tilde{B}$, then

$$\mathrm{var}[\tilde{A}] = E\left[\tilde{A}^2\right] - E[\tilde{A}]^2 = E\left[\tilde{A}^2\right] - \bar{A}^2 \tag{16}$$

and

$$\mathrm{cov}[\tilde{A}, \tilde{B}] = E[\tilde{A}\tilde{B}] - \bar{A}\bar{B}. \tag{17}$$

Note that the noise signal, $n(t)$, is the only random variable and is uncorrelated with the input, $x(t)$, and the noise-free output, $v(t)$. Also, the real and imaginary parts of the scaled discrete Fourier transforms of T seconds of $n(t)$, N_R and N_I, respectively, are uncorrelated:

$$E[N_R N_I] = 0 \tag{18}$$

and from Ref. [1, Section 9.1]

$$E\left[N_R^2\right] = E\left[N_I^2\right] = \left(\frac{T}{4}\right) G_{nn}, \tag{19}$$

where G_{nn} is the one-sided power spectral density of the noise signal. Using the same notation as Bendat and Piersol [1], the smoothed estimate, $\hat{G}_{nn}$, of G_{nn} is generated from an ensemble average

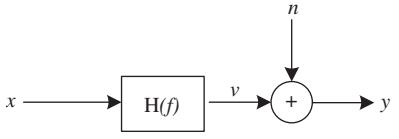

Fig. 3. System model with output noise only.

of n_{rec} independent sample records. The resulting sample covariance matrix between the spectral components is

$$\mathbf{s}\left(\hat{G}_{xx},\hat{G}_{yy},\hat{C}_{xy},\hat{Q}_{xy}\right)=\begin{bmatrix}0 & 0 & 0 & 0\\ 0 & \dfrac{\left(1-\left(\hat{\gamma}_{xy}^2\right)^2\right)\hat{G}_{yy}^2}{n_{\text{rec}}} & \dfrac{\left(1-\hat{\gamma}_{xy}^2\right)\hat{G}_{yy}\hat{C}_{xy}}{n_{\text{rec}}} & \dfrac{\left(1-\hat{\gamma}_{xy}^2\right)\hat{G}_{yy}\hat{Q}_{xy}}{n_{\text{rec}}}\\ 0 & \dfrac{\left(1-\hat{\gamma}_{xy}^2\right)\hat{G}_{yy}\hat{C}_{xy}}{n_{\text{rec}}} & \dfrac{\left(1-\hat{\gamma}_{xy}^2\right)\hat{G}_{xx}\hat{G}_{yy}}{2n_{\text{rec}}} & 0\\ 0 & \dfrac{\left(1-\hat{\gamma}_{xy}^2\right)\hat{G}_{yy}\hat{Q}_{xy}}{n_{\text{rec}}} & 0 & \dfrac{\left(1-\hat{\gamma}_{xy}^2\right)\hat{G}_{xx}\hat{G}_{yy}}{2n_{\text{rec}}}\end{bmatrix}, \tag{20}$$

where $\hat{\gamma}_{xy}^2=|\hat{G}_{xy}|^2/(\hat{G}_{xx}\hat{G}_{yy})$ is the estimate of the ordinary coherence function, $\hat{G}_{xx}$ and $\hat{G}_{yy}$ are the smoothed estimates of the power spectral densities of the input and output signals, respectively, and $\hat{C}_{xy}$ and $\hat{Q}_{xy}$ are the estimates of the co- and quad-spectral densities. The cross-spectral density, $\hat{G}_{xy}$, is given by $\hat{G}_{xy}=\hat{C}_{xy}+\mathrm{j}\hat{Q}_{xy}$. A convenient feature of this model is that the sample covariance matrix can be estimated from just the measurement of the input signal and the output signal. Note that because the excitation signal is deterministic and periodic, there is no variation in the power spectral density of either the input or the noise-free output. This is reflected by the row and column of zeros in Eq. (20). The other two zeros in the sample covariance matrix show that the co- and quad- spectral densities are also uncorrelated to each other. The remaining nonzero elements quantify the variance, if on the diagonal, and the covariance, if off the diagonal.

The uncertainty in the frequency response function is found by using a multivariate method to propagate the uncertainty from the spectral estimates given in Eq. (20) to the frequency response function estimator. The unbiased estimator of the frequency response function for this system model is [1,21]

$$\hat{H}_1=\frac{\hat{G}_{xy}}{\hat{G}_{xx}} \tag{21}$$

or using real and imaginary forms that are more convenient for the multivariate method

$$\begin{bmatrix}\hat{H}_{1,R}\\ \hat{H}_{1,I}\end{bmatrix}=\begin{bmatrix}\hat{C}_{xy}/\hat{G}_{xx}\\ \hat{Q}_{xy}/\hat{G}_{xx}\end{bmatrix}. \tag{22}$$

With the data reduction equation defined, the Jacobian matrix becomes

$$\mathbf{J}_{H_1}=\begin{bmatrix}\dfrac{\partial H_{1R}}{\partial G_{xx}} & \dfrac{\partial H_{1R}}{\partial G_{yy}} & \dfrac{\partial H_{1R}}{\partial C_{xy}} & \dfrac{\partial H_{1R}}{\partial Q_{xy}}\\ \dfrac{\partial H_{1I}}{\partial G_{xx}} & \dfrac{\partial H_{1I}}{\partial G_{yy}} & \dfrac{\partial H_{1I}}{\partial C_{xy}} & \dfrac{\partial H_{1I}}{\partial Q_{xy}}\end{bmatrix}=\begin{bmatrix}-\dfrac{\hat{C}_{xy}}{\hat{G}_{xx}^2} & 0 & \dfrac{1}{\hat{G}_{xx}} & 0\\ -\dfrac{\hat{Q}_{xy}}{\hat{G}_{xx}^2} & 0 & 0 & \dfrac{1}{\hat{G}_{xx}}\end{bmatrix}. \tag{23}$$

Thus, the sample covariance matrix for the estimate of the frequency response function is given by Eq. (9):

$$\mathbf{s}\left(\hat{H}_{1,R},\hat{H}_{1,I}\right)=\begin{bmatrix}\dfrac{\left(1-\hat{\gamma}_{xy}^2\right)\hat{G}_{yy}}{2n_{\text{rec}}\ \hat{G}_{xx}} & 0\\ 0 & \dfrac{\left(1-\hat{\gamma}_{xy}^2\right)\hat{G}_{yy}}{2n_{\text{rec}}\ \hat{G}_{xx}}\end{bmatrix}. \tag{24}$$

Eq. (24) gives the standard uncertainty that is used to propagate the uncertainty in the frequency response function through any subsequent data reduction equation. Using Eqs. (9) and (11) and simplifying gives the

polar form of the uncertainty

$$\mathbf{s}\left(\left|\hat{H}_1\right|, \angle\hat{H}_1\right) = \begin{bmatrix} \dfrac{\left(1-\gamma_{xy}^2\right)}{2n_{\text{rec}}\,\gamma_{xy}^2}\left|\hat{H}_1\right|^2 & 0 \\ 0 & \dfrac{\left(1-\gamma_{xy}^2\right)}{2n_{\text{rec}}\,\gamma_{xy}^2} \end{bmatrix}. \tag{25}$$

The square root of the diagonal terms in Eq. (25) exactly match those given in Table 9.6 in Bendat and Piersol [1], thus validating the multivariate technique used to derive those expressions. This approach is extended in the next section to a more complex system model where expressions for the uncertainty are not available in the literature.

Eq. (25) shows that the uncertainty in the frequency response function is related to the number of spectral averages, the ordinary coherence function, and the magnitude of the frequency response function itself. Increasing the value of the ordinary coherence function will lower the standard uncertainty in the frequency response function. This can be accomplished by designing the measurement to reduce any nonlinearities and noise sources. Increasing the number of averages will also decrease the sample covariance matrix but only reduces the standard uncertainties as $\propto 1/\sqrt{n_{\text{rec}}}$.

3.2. Uncorrelated input/output noise system model

The second model, with uncorrelated noise added to the input and output signals, is shown in Fig. 4. An example of such a system is the measurement of the mechanical impedance or admittance of a structure. Here, where u is the pseudo-random input signal, v is the noise-free output of the system, m and n are uncorrelated, zero-mean, Gaussian noise signals, x is the measured input signal, y is the measured output signal, and $H(f)$ is the frequency response function of the system. Again, the noise signals account for measurement noise and unmodeled dynamics. This model is appropriate for systems in which an input signal is supplied to an actuator that excites the system, and the outputs of the actuator (instead of the function generator) and the system are both measured.

The measured noise corrupted input signal is

$$x(t) = u(t) + m(t), \tag{26}$$

where $u(t)$ is a periodic-random excitation signal with period T. Using the notation described earlier, Eq. (26) can be transformed to the frequency domain yielding

$$X\left(f_k, T\right) = U\left(f_k, T\right) + M\left(f_k, T\right). \tag{27}$$

As in the first case,

$$y(t) = v(t) + n(t) = h(t)^* u(t) + n(t) \tag{28}$$

and, due to the periodic nature of the excitation

$$Y\left(f_k, T\right) = V\left(f_k, T\right) + N\left(f_k, T\right) = H\left(f_k, T\right) U\left(f_k, T\right) + N\left(f_k, T\right). \tag{29}$$

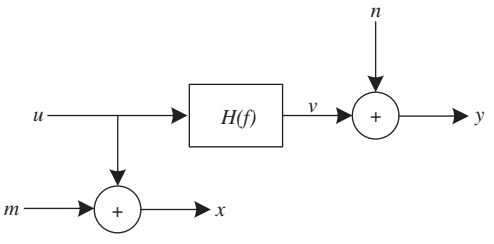

Fig. 4. System model of a system with uncorrelated input/output noise.

Denote the real and imaginary parts of $M(f_k, T)$ and $N(f_k, T)$ as M_R and M_I and N_R and N_I, respectively. The expressions for the random uncertainty and the variance are derived in a similar manner as before. One important note for this case is the assumption of uncorrelated noise sources. Since m and n are assumed to be uncorrelated, the cross-spectral density function between them is identically zero. This fact is used to simplify the variance and covariance expressions along with the expressions for the expectations of two zero-mean, Gaussian signals given in Eqs. (18) and (19), with corresponding version for m, and with

$$E[M_R N_R] = E[M_I N_I] = \left(\frac{T}{4}\right) C_{mn} = 0 \tag{30}$$

and

$$E[M_R N_I] = -E[M_I N_R] = \left(\frac{T}{4}\right) Q_{mn} = 0 \tag{31}$$

all provided in Section 9.1 of [1], where $\hat{C}_{mn}$ and $\hat{Q}_{mn}$ are the co- and quad-spectral density of the two noise signals. The simplified result for the estimate of the sample covariance matrix is

$$\mathbf{s}\left(\hat{G}_{xx}, \hat{G}_{yy}, \hat{C}_{xy}, \hat{Q}_{xy}\right) = \begin{bmatrix} \dfrac{\hat{G}_{mm}\left(2\hat{G}_{xx} - \hat{G}_{mm}\right)}{n} & 0 & \dfrac{\hat{G}_{mm}\hat{C}_{xy}}{n} & \dfrac{\hat{G}_{mm}\hat{Q}_{xy}}{n} \\ 0 & \dfrac{\hat{G}_{nn}\left(2\hat{G}_{yy} - \hat{G}_{nn}\right)}{n} & \dfrac{\hat{G}_{nn}\hat{C}_{xy}}{n} & \dfrac{\hat{G}_{nn}\hat{Q}_{xy}}{n} \\ \dfrac{\hat{G}_{mm}\hat{C}_{xy}}{n} & \dfrac{\hat{G}_{nn}\hat{C}_{xy}}{n} & \dfrac{\psi}{2n} & 0 \\ \dfrac{\hat{G}_{mm}\hat{Q}_{xy}}{n} & \dfrac{\hat{G}_{nn}\hat{Q}_{xy}}{n} & 0 & \dfrac{\psi}{2n} \end{bmatrix}, \tag{32}$$

where $\psi = \hat{G}_{nn}\hat{G}_{xx} + \hat{G}_{mm}\hat{G}_{yy} - \hat{G}_{mm}\hat{G}_{nn}$, $\hat{G}_{mm}$ is an estimate of the power spectral density of the input noise signal, and $\hat{G}_{nn}$ is an estimate of the power spectral density of the output noise signal. The zero elements $(1, 2)$ and $(2, 1)$ in Eq. (32) show that the estimates of the power spectral density for the input signal and output signal are uncorrelated, a consequence of the deterministic nature of $x(t)$. Similarly, the zero elements $(3, 4)$ and $(4, 3)$ in Eq. (32) show that the co- and quad-spectral densities are again uncorrelated. Note that this system is *not* completely characterized by measurements of just the input and output signals, because estimates of $\hat{G}_{mm}$ and $\hat{G}_{nn}$ are also required to calculate the sample covariance matrix. In practice, these can be estimated by either measuring the input and output signals when the source is turned off, thus setting $u = 0$, or by using application-specific noise models. With no input signal, the measured quantities arise solely due to the noise. Inherent to this approach is the assumption that the addition of the input signal does not change the estimates of the noise power spectra. The covariance matrix due to the random uncertainty can also be accurately estimated from computing the statistics directly from repeated measurements of the spectral density functions. This approach will account for any changes in the amplitudes of the noise signals due to the presence of the excitation signal. The drawback to this approach is the requirement to obtain and store each spectral quantity needed to compute the covariance matrix; these are not normally supplied by signal analyzers.

To propagate the uncertainty to the frequency response function, a form of the frequency response function must be chosen. The estimator for the frequency response function used in the remainder of this paper is $\hat{H}_3$, defined as [21]

$$\hat{H}_3 = \frac{\hat{G}_{xy}}{\sqrt{\hat{G}^*_{xy}\,\hat{G}_{xy}}} \sqrt{\frac{\hat{G}_{yy}}{\hat{G}_{xx}}}. \tag{33}$$

This definition of the frequency response function estimator is one of the popular choices in the ISO standard for the two-microphone method for acoustic impedance testing [22]. Substituting in the definitions for the spectral densities, Eq. (33) becomes

$$\hat{H}_3 = H\sqrt{\frac{1+\hat{G}_{nn}/\hat{G}_{vv}}{1+\hat{G}_{mm}/\hat{G}_{uu}}}. \tag{34}$$

Eq. (34) shows that $\hat{H}_3$ is biased, but if the input and output noise-to-signal ratios are either both small or non-negligible but the same order of magnitude, these biases tend to cancel each other, providing a better estimate of the frequency response function in the case with two uncorrelated noise sources [21]. Other estimators for the frequency response function are available as described in Refs. [5,21,23], each with its own advantages and disadvantages. The specific choice will depend on the requirements of the measurement and the ultimate final use of the data.

The resulting form of $\hat{H}_3$ for the multivariate uncertainty analysis is

$$\begin{bmatrix} \hat{H}_{3,R} \\ \hat{H}_{3,I} \end{bmatrix} = \begin{bmatrix} \sqrt{\dfrac{\hat{G}_{yy}}{\hat{G}_{xx}\left(\hat{C}_{xy}^2+\hat{Q}_{xy}^2\right)}}\,\hat{C}_{xy} \\ \sqrt{\dfrac{\hat{G}_{yy}}{\hat{G}_{xx}\left(\hat{C}_{xy}^2+\hat{Q}_{xy}^2\right)}}\,\hat{Q}_{xy} \end{bmatrix}. \tag{35}$$

The Jacobian matrix for $\hat{H}_3$ is

$$\mathbf{J}_{H_3} = \begin{bmatrix} -\sqrt{\dfrac{\hat{G}_{yy}}{\hat{G}_{xx}}}\dfrac{\hat{C}_{xy}}{2\hat{G}_{xx}\left|\hat{G}_{xy}\right|} & \dfrac{\hat{C}_{xy}}{2\sqrt{\hat{G}_{xx}\hat{G}_{yy}\left|\hat{G}_{xy}\right|^2}} & \sqrt{\dfrac{\hat{G}_{yy}}{\hat{G}_{xx}}}\dfrac{\hat{Q}_{xy}^2}{\left|\hat{G}_{xy}\right|^3} & -\sqrt{\dfrac{\hat{G}_{yy}}{\hat{G}_{xx}}}\dfrac{\hat{C}_{xy}\hat{Q}_{xy}}{\left|\hat{G}_{xy}\right|^3} \\ -\sqrt{\dfrac{\hat{G}_{yy}}{\hat{G}_{xx}}}\dfrac{\hat{Q}_{xy}}{2\hat{G}_{xx}\left|\hat{G}_{xy}\right|} & \dfrac{\hat{Q}_{xy}}{2\sqrt{\hat{G}_{xx}\hat{G}_{yy}\left|\hat{G}_{xy}\right|^2}} & -\sqrt{\dfrac{\hat{G}_{yy}}{\hat{G}_{xx}}}\dfrac{\hat{C}_{xy}\hat{Q}_{xy}}{\left|\hat{G}_{xy}\right|^3} & \sqrt{\dfrac{\hat{G}_{yy}}{\hat{G}_{xx}}}\dfrac{\hat{C}_{xy}^2}{\left|\hat{G}_{xy}\right|^3} \end{bmatrix}, \tag{36}$$

where $|\hat{G}_{xy}| = \sqrt{\hat{C}_{xy}^2+\hat{Q}_{xy}^2}$. From Eq. (36) it can be seen that the uncertainty in $\hat{H}_3$ scales with $\sqrt{\hat{G}_{yy}/\hat{G}_{xx}}$. Thus, the uncertainty increases at resonance where the output is large for a small input. The opposite may appear to be true at an anti-resonance, in this case the output signal is low, and this measurement condition is often dominated by noise.

The Jacobian matrix in Eq. (36) and the sample covariance matrix in Eq. (32) are cumbersome and do not result in a compact analytical expression. A suitable option is to evaluate each term numerically and then use matrix multiplication as required by Eq. (9). The 95% simultaneous confidence intervals for each variate are then estimated by taking the square root of the diagonal element and multiplying by the coverage factor computed from Eq. (6), with two variates and the correct effective number of degrees of freedom.

A numerical simulation is performed to verify the expressions derived in this section. A normalized two degree of freedom system model is chosen for the numerical simulations to represent a system with a known frequency response function. The model of the frequency response function is

$$H = \frac{1-(f/f_1)^2+\mathrm{j}2\zeta_1(f/f_1)}{\left(1-(f/f_2)^2+\mathrm{j}2\zeta_2(f/f_2)\right)\left(1-(f/f_3)^2+\mathrm{j}2\zeta_3(f/f_3)\right)}, \tag{37}$$

where f is the frequency, f_2 and f_3 are the undamped natural frequencies with corresponding damping ratios, ζ_2 and ζ_3, respectively. Similarly, a trough in the magnitude of the frequency response function is modeled via an undamped anti-resonance f_1 with a damping ratio ζ_1. The values of the parameters chosen for the simulations are $f_1 = 20\,\mathrm{Hz}$, $f_2 = 10\,\mathrm{Hz}$, $f_3 = 30\,\mathrm{Hz}$, $\zeta_1 = 0.05$, $\zeta_2 = 0.2$, and $\zeta_3 = 0.05$, as a matter of convenience. The spectral analysis is performed with 1000 sample records of data with 1024 samples each, and the Nyquist

frequency is set to 128 Hz. The pseudo-random noise signal is constructed as the summation of 512 sine wave components with frequencies at multiplies of 0.25 Hz. The DC component was set to zero. Each sine wave component has unit amplitude and the power in the input noise signal is 2.56×10^{-2} units squared and the power in the output noise signals is 2.5×10^{-3} units squared. The overall signal-to-noise ratio is thus 40 dB for the input signal, x, and is 45 dB for the output signal, y. A uniform window with no overlap is used for the spectral analysis.

The procedure of the simulation is as follows. First, one block (period) of the noise-free pseudo-random noise signal is generated. One period of the steady-state (periodic) response is generated by scaling the Fourier series coefficients of the input signal by the frequency response function's value at the frequency of the Fourier series component. Independent, zero-mean, Gaussian noise signals were added to both noise-free signals in the time domain. The spectral quantities are then computed and $\hat{H}_3$ is estimated by using Eq. (35). This procedure is repeated for each of the 1000 sample records. Finally, the uncertainties are computed by using the results of this section via the multivariate method, as well as directly from the statistics of the 1000 sample records.

The estimated frequency response function from the simulation is shown in Fig. 5. The results for this simulation are limited to the frequency range of 0–60 Hz to avoid the bias error described in Eq. (34). The modeled system attenuates the output signal at higher frequencies, thus the signal-to-noise ratio of the output signal will decrease because the power in the noise signal is assumed to be constant across all frequencies. By limiting the results to 60 Hz, the bias error in the estimated frequency response function is less than 0.15%. The uncertainty estimates are not shown in Fig. 5 for clarity but are plotted in Fig. 6, the results from both the multivariate method and the statistics calculated from the simulations are shown. The distribution of the 1000 raw averages is a bivariate normal distribution, thus the confidence region is assumed to be symmetric and is computed by estimating the sample covariance matrix and applying the coverage factor to the square root of the diagonal elements. The value of the 95% coverage factor is 2.45 and is computed from Eq. (6). The results of using the two methods to estimate the uncertainty are essentially indistinguishable in Fig. 6. The largest difference between the two uncertainty methods is 5% for the magnitude and 1.1×10^{-2} degrees for the phase and the average difference is 1.5% for the magnitude and 1.3×10^{-3} degrees for the phase. The true value of the frequency response function falls outside the uncertainty range at only 5 frequency bins for the magnitude

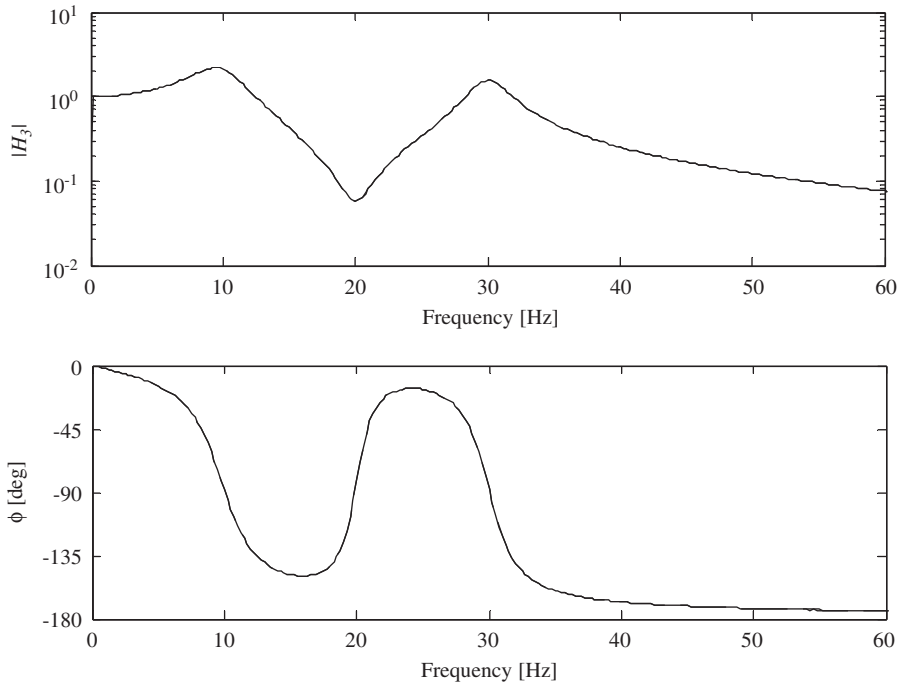

Fig. 5. Bode plot of the true frequency response function and the experimental estimate. ——, Frequency response function estimate, — —, true frequency response function. The true and estimated frequency response function are indistinguishable.

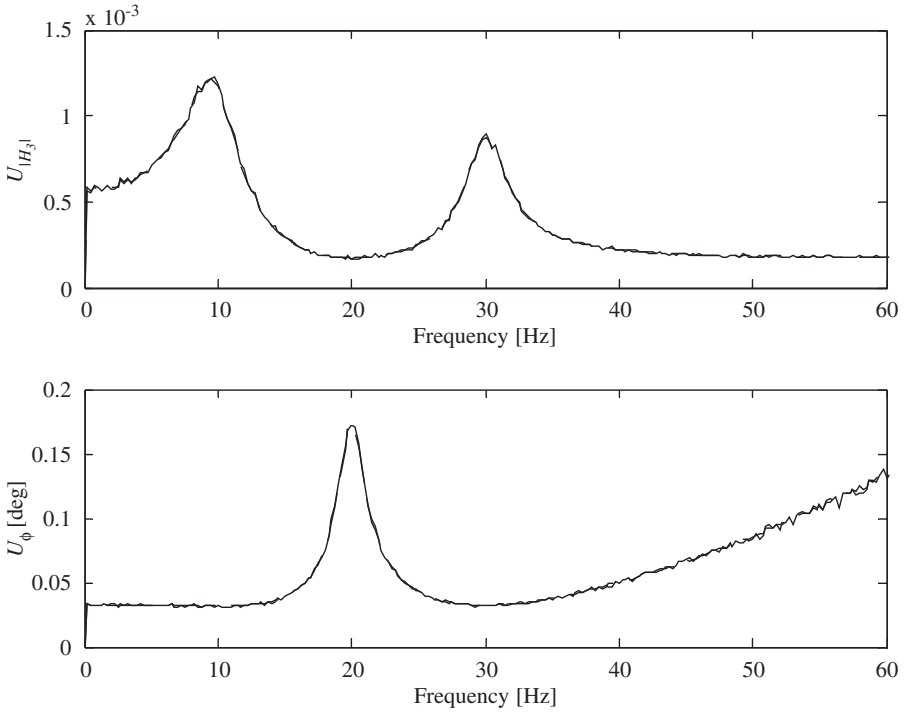

Fig. 6. Magnitude and phase plot of the uncertainty estimates. ——, Multivariate method, — —, direct computation. The two methods to estimate the uncertainty are essentially indistinguishable.

and only 7 frequency bins for the phase. Under the assumption that for a linear system, each frequency bin is independent, the estimated value of the frequency response function is consistent with a 95% confidence interval.

The plot of the uncertainty estimates shows that the maximum uncertainty in the magnitude is at the resonance frequencies, and the minimum is at the anti-resonance frequency. The maximum uncertainty in the phase of the frequency response function is at the anti-resonance. At least one of the signals from the transducers used to measure the input and output from the system may be noisy near a peak (system resonance) or a trough (system anti-resonance) in the magnitude of the frequency response function. From Fig. 6, it can also be seen the uncertainty in the phase angle continues to increase as the frequency is increased. This reveals that at high frequencies the uncertainty in the phase angle may be dominant and may determine the accuracy and number of spectral averages needed to obtain the desired uncertainty in the frequency response function estimate.

4. Application: measurement of the frequency response function between two microphones in a waveguide

The multivariate uncertainty method is now demonstrated on actual experimental data in an important acoustic application. The two-microphone method is the standard technique for measuring the specific acoustic impedance of a material specimen [22,24]. This method uses a waveguide with a compression driver mounted at one end, while the specimen is mounted at the other end. Two microphones are flush mounted to the side of the waveguide at two different axial locations. The compression driver is typically excited with a broadband signal, such as a pseudo-random noise signal, to produce plane traveling waves within the waveguide over a limited frequency range. The incident waves reflect off the specimen mounted at the end and create a standing wave pattern. The frequency response function is measured between the two microphones and a data reduction equation is then used to compute the acoustic properties of the specimen from the frequency response function and a few other measurements, such as the temperature and the locations of the microphones. To estimate the uncertainty in the computed acoustic properties, such as the complex-valued

reflection coefficient, the uncertainty in the frequency response function must first be known. In this section, the uncertainty will be estimated by using the multivariate method and via direct computation of the statistics of the results of several repeats of the experiment.

The two measured acoustic signals are assumed to be corrupted by uncorrelated Gaussian noise. One of the microphones is assigned to be the input signal, and the other is assigned to be the output signal. Therefore, both the input and output signals contain noise, and the appropriate system model is that shown in Fig. 4.

The measurement of the frequency response function is subject to random and bias errors, the latter of which is primarily due to calibration errors in the two measurement channels when a periodic excitation signal is used. To remove this bias, measurements are taken in the original and switched positions [22,23]. The original frequency response function estimate, $\hat{H}^O$, and the switched frequency response function estimate, $\hat{H}^S$, are geometrically averaged to remove the calibration bias, resulting in

$$\hat{H} = \sqrt{\frac{\hat{H}^O}{\hat{H}^S}}. \tag{38}$$

An appropriate form of the real and imaginary part of $\hat{H}$ for the multivariate method is

$$\hat{H} = \begin{bmatrix} \dfrac{\left(\left(\hat{H}_R^O\right)^2 + \left(\hat{H}_I^O\right)^2\right)^{1/4}}{\left(\left(\hat{H}_R^S\right)^2 + \left(\hat{H}_I^S\right)^2\right)^{1/4}} \cos(\theta) \\ \dfrac{\left(\left(\hat{H}_R^O\right)^2 + \left(\hat{H}_I^O\right)^2\right)^{1/4}}{\left(\left(\hat{H}_R^S\right)^2 + \left(\hat{H}_I^S\right)^2\right)^{1/4}} \sin(\theta) \end{bmatrix}, \tag{39}$$

where

$$\theta = \frac{\tan^{-1}\left(\hat{H}_I^O/\hat{H}_R^O\right) - \tan^{-1}\left(\hat{H}_I^S/\hat{H}_R^S\right)}{2}. \tag{40}$$

The uncertainty in $\hat{H}$ can be estimated by calculating the uncertainty in the original and switched estimates and then propagating the result to $\hat{H}$ using the multivariate method. The input sample covariance matrix is formed by applying Eqs. (32) and (36) to each of the frequency response function in the original, $\mathbf{s}_{\hat{H}^O}$, and switched positions, $\mathbf{s}_{\hat{H}^S}$, to form their respective sample covariance matrices as outlined in Section 3.2. The two sample covariance matrices are formed into a single input covariance matrix as

$$\mathbf{s}_{\hat{H}} = \begin{bmatrix} \mathbf{s}_{\hat{H}^O} & \mathbf{0} \\ \mathbf{0} & \mathbf{s}_{\hat{H}^S} \end{bmatrix}, \tag{41}$$

where $\mathbf{0}$ is the zero matrix. The Jacobian for Eq. (39) is

$$J_{\hat{H}} = \begin{bmatrix} \dfrac{A_{1,1}}{2\left|\hat{H}^O\right|^{3/2}\left|\hat{H}^S\right|^{1/2}} & \dfrac{A_{1,2}}{2\left|\hat{H}^O\right|^{3/2}\left|\hat{H}^S\right|^{1/2}} & \dfrac{\left|\hat{H}^O\right|^{1/2}}{2\left|\hat{H}^S\right|^{5/2}}A_{1,3} & \dfrac{\left|\hat{H}^O\right|^{1/2}}{2\left|\hat{H}^S\right|^{5/2}}A_{1,4} \\ \dfrac{A_{2,1}}{2\left|\hat{H}^O\right|^{3/2}\left|\hat{H}^S\right|^{1/2}} & \dfrac{A_{2,2}}{2\left|\hat{H}^O\right|^{3/2}\left|\hat{H}^S\right|^{1/2}} & \dfrac{\left|\hat{H}^O\right|^{1/2}}{2\left|\hat{H}^S\right|^{5/2}}A_{2,3} & \dfrac{\left|\hat{H}^O\right|^{1/2}}{2\left|\hat{H}^S\right|^{5/2}}A_{2,4} \end{bmatrix}, \tag{42}$$

where $|\hat{H}^O| = \sqrt{\left(\hat{H}_R^O\right)^2 + \left(\hat{H}_I^O\right)^2}$, $|\hat{H}^S| = \sqrt{\left(\hat{H}_R^S\right)^2 + \left(\hat{H}_I^S\right)^2}$, and

$$\begin{aligned} A_{1,1} &= \hat{H}_R^O \cos(\theta) + \hat{H}_I^O \sin(\theta), & A_{2,1} &= -\hat{H}_I^O \cos(\theta) + \hat{H}_R^O \sin(\theta), \\ A_{1,2} &= \hat{H}_I^O \cos(\theta) - \hat{H}_R^O \sin(\theta), & A_{2,2} &= \hat{H}_R^O \cos(\theta) + \hat{H}_I^O \sin(\theta), \\ A_{1,3} &= -\hat{H}_R^S \cos(\theta) - \hat{H}_I^S \sin(\theta), & A_{2,3} &= \hat{H}_I^S \cos(\theta) - \hat{H}_R^S \sin(\theta), \\ A_{1,4} &= -\hat{H}_I^S \cos(\theta) + \hat{H}_R^S \sin(\theta), & A_{2,4} &= -\hat{H}_R^S \cos(\theta) - \hat{H}_I^S \sin(\theta). \end{aligned} \tag{43}$$

The waveguide used in this experiment has a cross-section of 2.54 cm × 2.54 cm and a usable frequency range of 0.5–6.7 kHz. The acoustic pressure signals are measured using two Brüel and Kjær Type 4138 microphones and a Brüel and Kjær Pulse Analyzer data acquisition system with a 16-bit analog-to-digital converter and 24-bit digital-to-analog converter. The two microphone signals were sampled at a rate of 16,384 samples per second. Each record used in the spectral estimation is of duration 0.125 s (2048 points), and a total of 100 records (204,800 data points) were used in the estimation. A periodic pseudo-random excitation signal is generated by the Pulse system and amplified with a Techron Model 7540 power amplifier before application to the BMS H4590P compression driver. The microphones are calibrated with a Brüel and Kjær Type 4228 Pistonphone. The microphone that is initially mounted furthest from the specimen is considered the reference signal and is denoted the input signal, x. The excitation signal is then applied, and the amplifier gain is adjusted such that the sound pressure level at the reference microphone is approximately 120 dB (reference 20 μPa) for each frequency bin. Then the full-scale voltage on the two measurement channels of the Pulse system is adjusted to maximize the dynamic range of the data system. The excitation signal is turned off and the microphone signals are used to estimate the noise spectra. The excitation signal is turned on and the two microphone signals are recorded with the microphones in their original positions and switched positions.

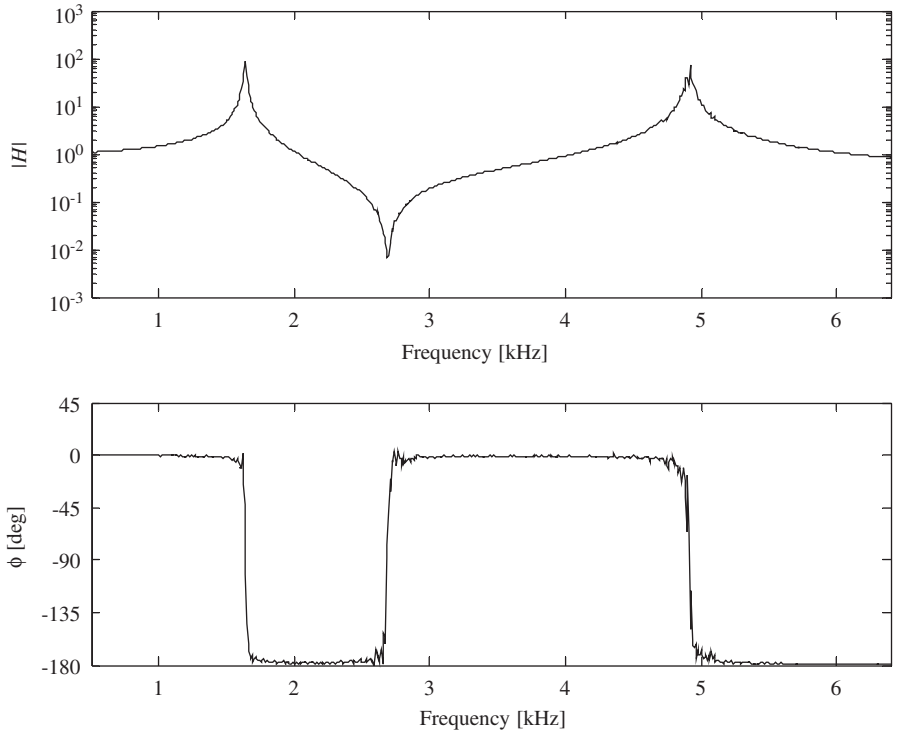

Fig. 7. The experimentally measured averaged frequency response function between the two microphones.

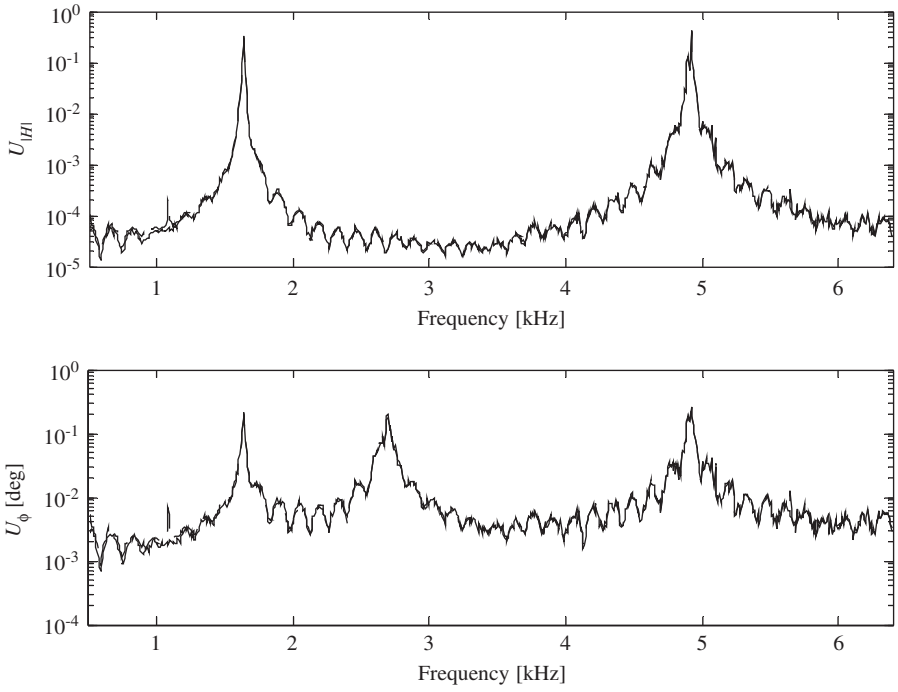

Fig. 8. Comparison for the uncertainty estimated by the multivariate method and by the direct statistics. — —, Direct statistics, ——, multivariate method. The two methods to estimate the uncertainty are essentially indistinguishable.

The time-series data are used to compute the power spectra and the cross-spectra between the two microphones for the original position and switched positions. The spectra are used to compute $\hat{H}_3$ by using Eq. (35) and the sample covariance matrices using Eq. (36). The computed frequency response function is shown in Fig. 7. The uncertainty in the spectral estimates is propagated to the magnitude and phase of the averaged frequency response function via the multivariate method by using Eq. (9) with Eqs. (41) and (42). The value of the 95% coverage factor for the averaged frequency response function is 2.50 and is computed from Eq. (6) using $n_{\mathrm{rec}}-1$ degrees of freedom, and the confidence intervals are computed from Eq. (5). Then the 100 sample estimates of the frequency response function are used to compute the sample covariance matrix between the magnitude and phase. The estimates of the uncertainty in the magnitude and phase are shown in Fig. 8. The uncertainty estimates agree well with each other except for at 1.65, 2.70, and 4.90 kHz, where one of the microphone locations corresponds to a node in the standing wave pattern. When this occurs, one of the microphones is measuring a small acoustic pressure, and the signal is dominated by the measurement noise. The value of the frequency response function will theoretically tend towards zero if the output microphone is at the node or will tend towards infinity if the input microphone is at the node. In both cases, the uncertainty in the frequency response function becomes large. The average difference between the two estimates of the simultaneous confidence intervals is 10% for the magnitude and 11% for the phase angle, and the maximum difference is 0.04 for the magnitude and 0.05° for the phase angle. Given the small number of records, these differences are deemed small enough to validate the multivariate uncertainty analysis.

5. Conclusions

An experimental measurement consists of two parts, an estimate of the measured quantity and an estimate of the uncertainty. The uncertainty allows users to determine whether or not the estimate is accurate enough for their needs. Classical methods for uncertainty analysis are restricted to scalar quantities and are not applicable to complex-valued frequency response function estimates, an important quantity in linear, time-invariant dynamic systems. The multivariate method extends the techniques of the classical method to

problems with any number of variates or dimensions. This paper applies the multivariate method to the nonparametric measurement of the frequency response function of a linear system. Two system models were considered, one with only noise in the output signal and the other with uncorrelated noise sources in both the input and output signals. The sample covariance matrices were derived for both cases for the spectral density estimates. The results showed that, in the first model, all required information is contained in the measurement of the input and output signals, while for the second model an extra measurement was required to estimate the power spectra of the two noise signals. The sample covariance matrices were then propagated to the magnitude and phase of the frequency response function. For the first model, the derived expressions for the uncertainty in the frequency response function were identical to published expressions in Bendat and Piersol [1, Table 9.6]. The second model was verified by numerical simulations, which showed that the multivariate method yielded uncertainty estimates consistent with the direct computation of the statistics from the sample records.

Finally, this paper demonstrated the multivariate method on real experimental data involving the frequency response estimation between two microphones in an acoustic waveguide. The estimate of the uncertainty by the multivariate method yielded consistent results with the direct computation of the statistics from the sample records. The results demonstrate that the multivariate method can be applied to experimental data that are multivariate in nature and provide reliable estimates of measurement uncertainty.

References

[1] J.S. Bendat., A.G. Piersol, *Random Data*, Wiley, New York, 2000, pp. 316–345, 425–431.
[2] H. Schmidt, Resolution bias errors in spectral density, frequency response and coherence function measurements, I–VI, *Journal of Sound and Vibration* 101 (3) (1985) 347–427.
[3] S. Gade, H. Herlufsen, *Windows to FFT Analysis*, Brüel and Kjær, Nærum, Denmark, 1987.
[4] R. Pintelon., J. Schoukens, *System Indentification: A Frequency Domain Approach*, IEEE, New York, 2001, pp. 33–68.
[5] R. Pintelon., J. Schoukens, Measurement of frequency response functions using periodic excitations, corrupted by correlated input/output errors, *IEEE Transactions on Instrumentation and Measurement* 50 (6) (2001) 1753–1760.
[6] R. Pintelon, Y. Rolain, W.V. Moer, Probability density function for frequency response function measurements using periodic signals, *IEEE Instrumentation and Measurement Technology Conference*, IEEE, Anchorage, AK, 21–23 May 2002.
[7] J. Schoukens, Y. Rolain, G. Simon, R. Pintelon, Fully automated spectral analysis of periodic signals, *IEEE Transactions on Instrumentation and Measurement* 52 (4) (2003) 1021–1024.
[8] B. Picinbono, *Random Signals and Systems*, Prentice-Hall, Englewood Cliffs, NJ, 1993.
[9] *Guide to the Expression of Uncertainty in Measurement*, International Organization for Standardization, Geneva, 1995.
[10] S.J. Kline, F.A. McClintock, Describing uncertainties in single-sample experiments, *Mechanical Engineering* 75 (1) (1953) 3–8.
[11] S.J. Kline, The purposes of uncertainty analysis, *Journal of Fluids Engineering* 107 (1985) 153–160.
[12] B.N. Taylor., C.E. Kuyatt, *Guidelines for Evaluating and Expressing the Uncertainty of NIST Measurement Results*, National Institute of Standards and Technology, Gaithersburg, MD, 1994.
[13] H.W. Coleman, W.G. Steele, *Experimentation and Uncertainty Analysis for Engineers*, second ed., Wiley, New York, 1999.
[14] B.D. Hall, Calculating measurement uncertainty for complex-valued quantities, *Measurement Science and Technology* 14 (2003) 368–375.
[15] B.D. Hall, On the propagation of uncertainty in complex-valued quantities, *Metrologia* 41 (2004) 173–177.
[16] N.M. Ridler, M.J. Salter, An approach to the treatment of uncertainty in complex S-parameter measurements, *Metrologia* 39 (2002) 295–302.
[17] R. Willink, B.D. Hall, A classical method for uncertainty analysis with multidimensional data, *Metrologia* 39 (2002) 361–369.
[18] R.J. Moffat, Using uncertainty analysis in the planning of an experiment, *Journal of Fluids Engineering* 107 (1985) 173–178.
[19] R.A. Johnson, D.W. Wichern, *Applied Multivariate Statistical Analysis*, fifth ed., Prentice-Hall, Upper Saddle River, NJ, 2002.
[20] R.B. Randall, *Frequency Analysis*, Brüel and Kjær, Nærum, Denmark, 1987.
[21] H. Vold, J. Crowley, G.T. Rocklin, New ways of estimating frequency response functions, *Journal of Sound and Vibration* (1984) 34–38.
[22] International Organization for Standardization ISO 10534-2:1998, Acoustics-determination of sound absorption coefficient and impedance in impedance tubes—part 2: transfer-function method, 1998.
[23] P.R. White, M.H. Tan, J.K. Hammond, Analysis of the maximum likelihood, total least squares and principle component approaches for the frequency response function estimation, *Journal of Sound and Vibration* 290 (2006) 676–689.
[24] ASTM International ASTM E1050-98, Impedance and absorption of acoustical materials using a tube, two microphones and digital frequency analysis system, 1998.